

General optical metrology for the dipole orientation in organic light-emitting diodes

Lingjie Fan,^{1,2} Ang Chen,² Tongyu Li,^{1,2} Haiwei Yin,² Lei Shi,^{1,2,3,*} and Jian Zi^{1,3,†}

¹Department of Physics, Key Laboratory of Micro- and Nano-Photonic Structures (Ministry of Education), and State Key Laboratory of Surface Physics, Fudan University, Shanghai 200433, China

²Shanghai Engineering Research Center of Optical Metrology for Nano-fabrication (SERCOM), Shanghai 200433, China

³Collaborative Innovation Center of Advanced Microstructures, Nanjing University, Nanjing 210093, China

(Dated: May 18, 2022)

Abstract

Considerable progress has been made in organic light-emitting diodes (OLEDs) to achieve high external quantum efficiency (EQE), among which the dipole orientation of OLED emitters has a remarkable effect. In most cases, EQE of the OLED emitter is theoretically predicted with only one orientation factor to match with corresponding experiments. Here, we develop a distribution theory with three independent parameters to fully describe the relationship between dipole orientations and power densities. Furthermore, we propose an optimal experiment configuration for measuring such distribution parameters. Measuring the unpolarized spectrum extremely can dig more information of dipole orientation distributions with a rather simple way. Our theory provides a universal plot of the OLED dipole orientation, paving the way for designing more complicated OLED structures.

PACS numbers: 42.79.-e

I. INTRODUCTION

Since the first reports of OLEDs in 1987¹, its efficiency has been improved through finding novel phosphorescent materials²⁻⁹, optimizing the thickness of each layer in the OLED stacks¹⁰⁻¹², and so on. In recent years, the emitting dipole orientation has also been drawing significant attention for enhancing light extraction from OLED stacks¹³⁻¹⁹.

The theory of dipole radiation in OLEDs originated from applying the theory of an electrical dipole near an interface to the problem of molecules fluorescing near a surface²⁰⁻²⁷. Recent researches on the dipole orientation have been proposed to enhance the EQE²⁸, in which the description of the dipole orientation distribution in the previous theory is applied. A dipole ensemble is decomposed into vertical dipole and horizontal dipole. The power radiated by the dipole ensemble is formed by weighting the power radiated by vertical dipole and horizontal dipole in a proportion. The scale factor, the ratio of vertical dipole and horizontal dipole, can be regarded as a parameter describing the vertical orientation distribution of the dipole ensemble.

Recently along with the OLED manufacturing progress increasingly, it is pointed out that a possible research direction of OLEDs in the future is to take advantage of the dipole ensemble with non-uniform horizontal orientation distribution²⁹. Some studies point out that the carrier mobility in films using the dipole ensemble perfect aligning in one direction is much higher than that of films using the uniform dipole ensemble^{30,31}. At the same time, other researchers show that OLEDs in which dipoles align in one direction can also achieve the emission of linear polarized light. Then, let the linear polarized light pass through a quarter-wave plate formed by the liquid crystal to realize the application of OLEDs directly emitting orthogonal circular polarized light³². Emitting dipole orientation is of great significance for the EQE, as well as the polarization. However, the previous works have so far considered the dipole ensemble with non-uniform vertical orientation distribution. With the further study of OLEDs and more precise control of the horizontal dipole orientation, there is no doubt that a theory fully describing the relationship between dipole orientation distribution and power density is needed.

Here, we develop a theory that fully describes the relationship between the orientation distribution of a dipole ensemble and its power density. In contrast to the decomposition method used in previous theories, we start from a dipole and consider an arbitrary distribu-

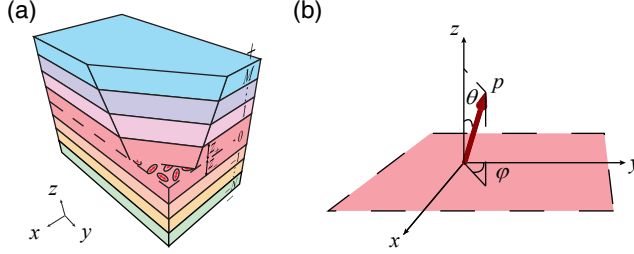


FIG. 1: (a) Sketch of the OLED stacks. The middle layer is the organic emitting layer, and its index of refraction and thickness are n_0 and d_0 , respectively. The emitting layer is sandwiched between two films with index of refraction n_i and thickness d_i . The distance between the position of the emitting dipoles and the upper interface of the emitting layer is z_+ . The outermost layers are semi-infinite layers. It is usually used to represent the environment outside the OLED stacks. The semi-infinite layers are labeled as $+$ and $-$. (b) The orientation of a dipole. The polar angle θ is the angle between the z axis and the dipole moment p , and the azimuth angle ϕ is the angle between the x axis and the dipole projection on the $x - y$ plane.

tion function, expressed as a Fourier series, to extend the power density of a dipole to the case of a dipole ensemble. Theoretically, it is strictly proved that only three independent distribution parameters are needed to fully describe the effect of orientation distribution of a dipole ensemble on its power density. Parameters a and b describe the vertical and horizontal orientation distribution, and parameter c describes the coupling between the vertical and horizontal distribution. Finally, using optical simulation, we design an experimentally feasible scheme for measuring these three distribution parameters, and present different spectra corresponding to different distribution parameters for the test structure.

II. DISTRIBUTION THEORY

The theoretical model of the OLED stacks is shown in Fig. 1(a). The emitting layer with an index of refraction n_0 and thickness d_0 is located between two stacks of layers. The intermediate layers $j1, j2, \dots$ have index of refraction n_{j1}, n_{j2}, \dots and d_{j1}, d_{j2}, \dots . The half-infinite spaces are labeled j ($j = 1, 2$). The dipole ensemble in layer 0 is located at a distance z_j from the interface at the j side of the layer. The OLED stacks, therefore, can be simplified to the multi-layer films. When there is only one electric dipole in the OLED stacks, whose

orientation is shown in FIG. 1(b) lower panel, its radiation can be characterized by the power density of a dipole $P(\theta, \phi)$. The detail expressions of the power density of a dipole in the OLED stacks are given in the appendix.

For a dipole ensemble with arbitrary orientation distribution in the OLED stacks, we use a distribution function $F(\theta, \phi)$ to describe its orientation distribution. Multiplied with distribution function and then integrated over the sphere with the polar angle θ and azimuth angle ϕ , the power density of a dipole can be used to describe a dipole ensemble:

$$P(a, b, c) = \int_0^{2\pi} \int_0^\pi P(\theta, \phi) F(\theta, \phi) d\theta d\phi, \quad (1)$$

where $P(a, b, c)$ is the power density of a dipole ensemble adjusted by three distribution parameters. The distribution parameters a , b , and c will be given through further derivation. The factor $\sin\theta$ in the spherical integral is included in distribution F for simplicity. Thus, the distribution function of dipole ensemble with three-dimensional isotropical random orientation distribution is given by:

$$F = \sin\theta \quad (2)$$

By using the Fourier series expansion, we can expand the distribution function $F(\theta, \phi)$ into Fourier series

$$F(\theta, \phi) = 1 + \sum_{m,n=1}^n (f_{m,n} \cos(2m\theta + n\phi) + g_{m,n} \sin(2m\theta + n\phi)), \quad (3)$$

with

$$f_{m,n} = \frac{2 \int_0^{2\pi} \int_0^\pi F(\theta, \phi) \cos(2m\theta + n\phi) d\theta d\phi}{\int_0^{2\pi} \int_0^\pi F(\theta, \phi) d\theta d\phi}, \quad (4a)$$

$$g_{m,n} = \frac{2 \int_0^{2\pi} \int_0^\pi F(\theta, \phi) \sin(2m\theta + n\phi) d\theta d\phi}{\int_0^{2\pi} \int_0^\pi F(\theta, \phi) d\theta d\phi}. \quad (4b)$$

Then, the arbitrary distribution function in the form of Fourier series is multiplied with the power densities of a dipole, and then is integrated over the polar angle and azimuth angle, as shown by Eq. (1). We find that only the integral values of four components are not zero among these integrations of the Fourier series, while the integral values of the rest components are all zero. These four components are controlled by three independent parameters. Therefore, the arbitrary distribution function can be simplified to a definite

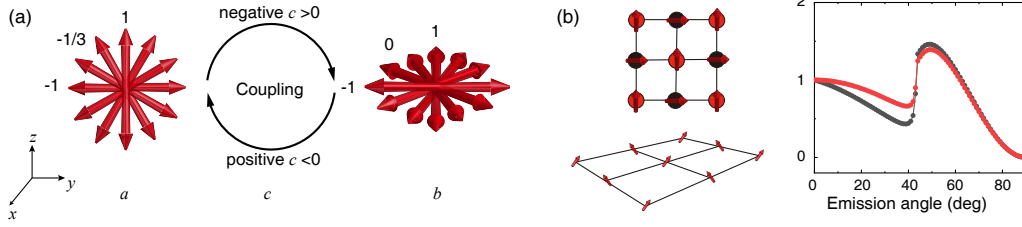


FIG. 2: (a) Intuitive physical meaning of distribution parameters a , b and c . The distribution parameters a and b describe the vertical and horizontal orientation distribution of the dipole ensemble, while the distribution parameter c describes the coupling effect. (b) A Specific distribution (left). The comparison of p -polarized spectra (right) obtained by previous decomposed method (red curve) and our distribution theory (black curve) for the specific distribution in the left.

three-parameter distribution function, given by

$$F(\theta, \phi) = 1 + 2a \cos 2\theta + 2b \cos 2\phi + 4c \sin 2\theta \cos \phi + 4d \cos 2\theta \cos 2\phi, \quad (5)$$

where the distribution parameter d is not an independent parameter. It is the product of the distribution parameters a and b

$$d = a \times b. \quad (6)$$

Since the integral values of these four distribution components can be calculated accordingly, the power densities per solid angle of a dipole ensemble with arbitrary orientation distribution, for an emission angle α in half-space j ($j = 1$), can be written as

$$P_1^s(a, b, c) = P^s \times \frac{1}{4}(1 - a - b + d), \quad (7a)$$

$$P_1^{p1}(a, b, c) = P_1^{p1} \times \frac{1}{2}(1 + a), \quad (7b)$$

$$P_1^{p2}(a, b, c) = P_1^{p2} \times \frac{1}{4}(1 - a + b - d), \quad (7c)$$

$$P_1^{p3}(a, b, c) = -P_1^{p3} \times \frac{c}{2}, \quad (7d)$$

with

$$P_1^s = \frac{k_1^2 \cos \alpha}{\pi} \frac{3}{8} \frac{1}{k_0 k_{z,0}} \frac{|1 + a_2^s|^2}{|1 - a^s|^2} T_1^s, \quad (8a)$$

$$P_1^{p1} = \frac{k_1^2 \cos \alpha}{\pi} \frac{3}{8} \frac{k_{\parallel}^2}{k_0^3 k_{z,0}} \frac{|1 + a_2^p|^2}{|1 - a^p|^2} T_1^p, \quad (8b)$$

$$P_1^{p2} = \frac{k_1^2 \cos \alpha}{\pi} \frac{3}{8} \frac{k_{z,0}}{k_0^3} \frac{|1 - a_2^p|^2}{|1 - a^p|^2} T_1^p, \quad (8c)$$

$$P_1^{p3} = -\frac{k_1^2 \cos \alpha}{\pi} \frac{3}{8} \frac{k_{\parallel}}{k_0^3} \frac{1}{|1 - a^p|^2} T_2^p T_1^p. \quad (8d)$$

III. INTUITIVE PHYSICAL MEANING

It is quite interesting and confusing that three independent parameters are needed to fully describe the orientation distribution of a dipole ensemble, instead of two parameters (θ, ϕ) . In the following, a specific distribution function F is studied to reveal the physical meaning of distribution parameters, especially parameter c .

In the case that there is only one dipole in the OLED stacks whose orientation is represented by (θ_1, ϕ_1) , the distribution function reads:

$$F(\theta, \phi) = \delta(\theta - \theta_1) \delta(\phi - \phi_1) \sin \theta. \quad (9)$$

Inserting Eqs. (9) into Eqs. (4), we can obtain the distribution parameters of a dipole:

$$a = \cos 2\theta_1, \quad (10a)$$

$$b = \cos 2\phi_1, \quad (10b)$$

$$c = \sin 2\theta_1 \cos \phi_1. \quad (10c)$$

The distribution parameters a , b , and c are controlled by two independent parameters (θ_1, ϕ_1) when there is only one dipole in the OLED stacks, which is consistent with common sense.

In the case that there are n dipoles in the OLED stacks whose orientations are represented by (θ_i, ϕ_i) , the distribution function reads:

$$F(\theta, \phi) = \sum_{i=1}^n (\delta(\theta - \theta_i) \delta(\phi - \phi_i) \sin \theta). \quad (11)$$

The same procedure may be easily adapted to obtain the distribution parameters of n

dipoles:

$$a = \frac{\sum_{i=1}^n (\sin \theta_i \cos 2\theta_i)}{\sum_{i=1}^n \sin \theta_i}, \quad (12a)$$

$$b = \frac{\sum_{i=1}^n (\sin \theta_i \cos 2\phi_i)}{\sum_{i=1}^n \sin \theta_i}, \quad (12b)$$

$$c = \frac{\sum_{i=1}^n (\sin \theta_i \sin 2\theta_i \cos \phi_i)}{\sum_{i=1}^n \sin \theta_i}. \quad (12c)$$

When there are n dipoles in the OLED stacks, distribution parameters a , b , and c are controlled by $2n$ independent parameters (θ_i, ϕ_i) . As shown by Eqs. (12), parameter a is adjusted by the weight $\cos 2\theta_i$, parameter b is adjusted by the weight $\cos 2\phi_i$, and parameter c is adjusted by the weight $\sin 2\theta_i \cos \phi_i$.

Therefore, parameters a and b describe the vertical and horizontal orientation distribution of a dipole ensemble respectively, and parameter c describes the coupling between the vertical and horizontal distribution, as illustrated in FIG. ??(a). The parameter a is used to describe the vertical distribution of a dipole ensemble. When $-1 \leq a < -1/3$, the orientation of a dipole ensemble tends to parallel to the horizontal $x - y$ plane; when $a = -1/3$, the orientation of a dipole ensemble is randomly distributed; when $-1/3 < a \leq 1$, the orientation of a dipole ensemble tends to parallel to z axis. The parameter b is used to describe the horizontal distribution of the dipole ensemble. When $-1 \leq b < 0$, the orientation of the dipole ensemble tends to parallel to the y axis, when $b = 0$, the orientation of the dipole ensemble is randomly distributed; when $0 < b \leq 1$, the orientation of the dipole ensemble tends to parallel to the x axis. The parameter c is used to describe the coupling. When $c < 0$, the coupling between the vertical and horizontal distribution is positive for the power densities increase as shown by Eq. (7d); when $c = 0$, there is no coupling and dipoles can be decomposed into vertical dipole and horizontal dipole which is wildly applied in the previous theories; when $c > 0$, the coupling effect is negative. For the distribution parameter a , it is related to Θ and S^{28} , previously used to describe the vertical orientation distribution of dipoles, given by

$$a = 1 - 2\Theta = \frac{1}{3}(1 + 4S). \quad (13)$$

We use a specific orientation distribution of nine dipoles to explain the difference between our distribution theory and the previous distribution theory. As illustrated in FIG. ??(b), the orientation of the dipole at the vertex and center is $(\pi/4, 0)$, and the orientation of the

dipole on the four sides is $(\pi/4, \pi/2)$. Its distribution function can be expressed as:

$$F(\theta, \phi) = 5\delta\left(\theta - \frac{\pi}{4}\right)\delta(\phi - 0)\sin\theta + 4\delta\left(\theta - \frac{\pi}{4}\right)\delta\left(\phi - \frac{\pi}{2}\right)\sin\theta. \quad (14)$$

The distribution parameters a , b , and c of the orientation distribution of nine dipoles in FIG. ??(b) are given by

$$a = 0, \quad b = \frac{1}{9}, \quad c = \frac{5}{9}. \quad (15)$$

By using Eqs. (7), we can obtain its p -polarized power density, which represents the data usually obtained in the experiment¹³, as shown in FIG. ??(b) (black curve). Then, the value of p -polarized power density are calculated using the formula describing the uniform horizontal distribution in the previous theory, as shown in FIG. ??(b) (red curve). Using a converging algorithm to reduce mean square error (MSE) between the black curve and red curve, we can obtain its vertical distribution parameters:

$$a = -0.09, \quad \Theta = 0.45, \quad S = -0.32. \quad (16)$$

The best match curve is shown in FIG. ??(b) (red). There is a significant mismatch between the black curve and red curve, which lead to deviations of the vertical distribution parameters obtained by spectrum fitting.

IV. PROPOSED EXPERIMENT CONFIGURATION

For determining the orientation distribution of the emitting dipole ensemble in the emitting layer, the test structure we considered is shown in FIG. 3(i). An organic thin film is evaporated on the glass substrate, whose thickness is d . The emitting dipoles are doped in the middle of the emitting layer. By measuring the intensity of the spectrum at different angles, we can get the intensity changing with respect to the emission angle. Then the intensity of the spectra at 0 emission angle is normalized to 1. These normalized spectra usually have different shapes, which indicate different orientation distribution of the emitting dipoles.

Since distribution parameter Θ or S was used in the previous study of emitting dipole orientation, only p -polarized spectra were considered in previous experiment configuration to measure the orientation distribution of the emitting dipole ensemble^{13,17}. However, non-polarized spectra should be used for analysis in our proposed experiment configuration, in

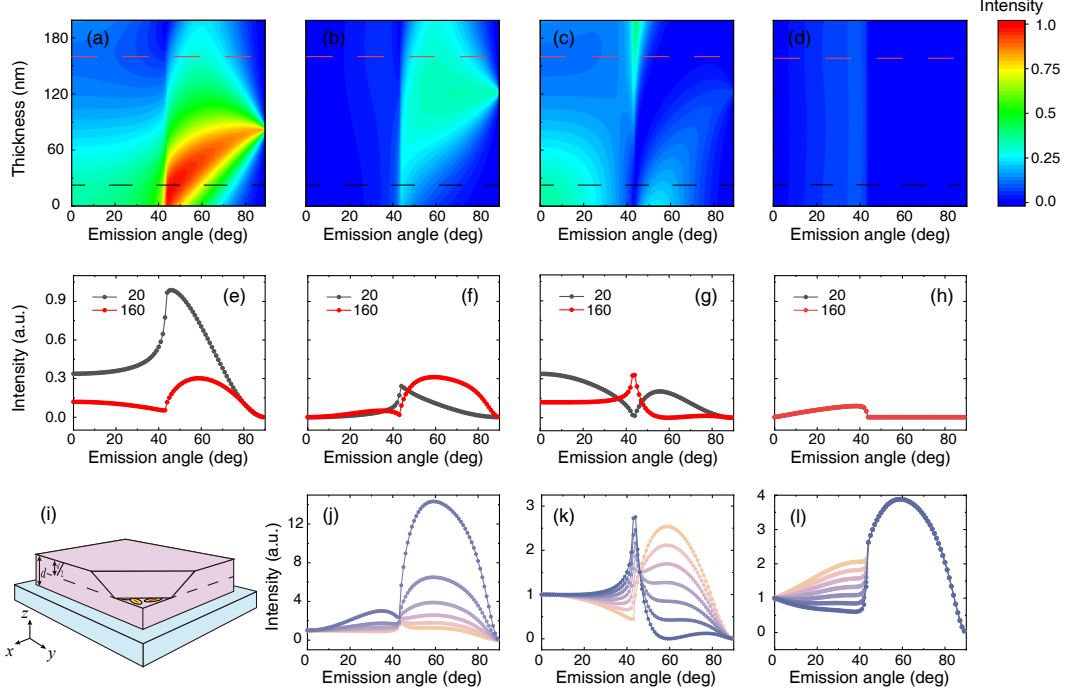


FIG. 3: (a)-(d) Simulated different energy densities P_1^s , P_1^{p1} , P_1^{p2} , and P_1^{p3} at different emission angle and different thickness. (e)-(d) The change of power density with emission angle at 20 nm and 160 nm.

order to contain all information of these three distribution parameters. The normalized non-polarized spectra consist of four components P_1^s , P_1^{p1} , P_1^{p2} , and P_1^3 , and they are adjusted by three independent parameters a , b , and c , as shown by Eqs. (7). If only normalized p -polarized spectra are used for analysis, the distribution parameter b cannot be obtained. At the same time, the use of non-polarized spectra also makes the experiment operation easier without precisely rotating the polarizer to the p -polarized direction in the experiment.

In our proposed experiment configuration, the use of non-polarized spectra requires us to consider s -polarized spectra on the basis of the previous analysis of p -polarized spectra. In order to distinguish the s -polarized power density and p -polarized power densities of different shapes, the thickness of the emitting layer should be optimized, as illustrated in FIG. 3(a)-(h). The s -polarized and p -polarized power densities P_1^s , P_1^{p1} , P_1^{p2} , and P_1^{p3} are supposed to be in different shapes but in the same order of magnitude. When the thickness of the emitting layer approaches 0, the s -polarized power density is much stronger than the p -polarized power densities. The p -polarized power densities have little effect on

the total power density, and the dipole orientation distribution information contained in the p -polarized power densities is easily concealed by the noise during the measurement. By increasing the thickness of the emitting layer, as shown in FIG 3(a), the s -polarized power density begins to decrease, and the p -polarized power densities begin to increase. The optimal thickness of the emitting layer is near 160 nm, where all four power densities have a significant impact on the total power density obtained by superposition. Finally, we design an optimal experiment configuration in which three distribution parameters could be measured precisely. When the thickness of the emitting layer is 160 nm, non-polarized spectra corresponding to different distribution parameters are shown in FIG. 3(j)-(l).

For an electric dipole, it hardly radiates to the direction of its dipole moment. As the distribution parameter a approaches 1, the orientation of the dipole moment tends to parallel to the z axis, and its intensity at 0 emission angle becomes weak. Thus, the normalized non-polarized spectra have stronger intensities at large emission angles, as illustrated in FIG. 3(j). This intuitive property of an electric dipole also leads to the anisotropy of its intensity when the horizontal orientation distribution of the dipole is anisotropic. When the orientation of dipole moment parallels to the x axis, its intensities in $x - z$ plane at large emission angles become weak. Therefore intensities in $x - z$ plane at large emission angles become weaker as the distribution parameter b approaches 1, shown in FIG. 3(k). Since the distribution parameter c is difficult to explain in an intuitive physical meaning, we have to refer to its mathematical form P_1^{p3} . As shown in Eq. (8), power density P_1^{p3} is formed by multiplying the forward energy transmission coefficient with the backward energy transmission coefficient. When the emission angle becomes larger, total internal reflection occurs at the interface between the air layer and the emitting layer and P_1^{p3} becomes 0. Therefore, the distribution parameter c only affects intensities where the emission angles are smaller than the total internal reflection angle, as illustrated in FIG. 3(l).

V. SUMMARY AND CONCLUSION

By introducing an arbitrary distribution function to expand a dipole into a dipole ensemble, we have rigorously proved that only three distribution parameters are needed to fully describe the relationship between the orientation distribution of a dipole ensemble and its power density. These three independent parameters could adjust the ratio of different parts

of the power density, which means that we can determine these three distribution parameters by measuring the power intensity radiated by the dipole ensemble in the OLED stacks.

We have discussed an optimal experiment configuration for measuring the three distribution parameters proposed in our distribution theory and intuitively explains the reason why these three distribution parameters a , b , and c could be obtained from the normalized non-polarized spectrum. With the improvement of OLED manufacturing technology and more precise control of the orientation of dipoles in OLED stacks, our method fully describes the orientation distribution of dipoles in OLED stacks, thereby providing guidance for OLED manufacturing technology.

We thank Xiaoyuan Hou and Shaobo Liu for useful discussions about experiment configuration, and Zhenghong Li for fruitful discussions. We acknowledge financial support by ...

Appendix A: The power density of a dipole in the stacks

For the multi-layer model shown in FIG.1(a), the energy reflection and transmission coefficients are given by

$$R_j^{s,p} = |r_j^{s,p}|^2 \quad \text{for all cases,} \quad (\text{A1a})$$

$$T_j^s = |t_j^s|^2 \frac{k_{z,j}}{|k_{z,0}|} \quad \text{for } \text{Im}(k_{z,j}) = 0, \quad (\text{A1b})$$

$$T_j^p = |t_j^p|^2 \frac{n_0^2}{n_j^2} \frac{k_{z,j}}{|k_{z,0}|} \quad \text{for } \text{Im}(k_{z,j}) = 0, \quad (\text{A1c})$$

$$T_j^{s,p} = 0 \quad \text{for } \text{Im}(k_{z,j}) \neq 0, \quad (\text{A1d})$$

where $r_j^{s,p}$, $t_j^{s,p}$ are Fresnel reflection and transmission coefficients. The energy coefficients and Fresnel coefficients with subscripts j represent the reflection and transmission coefficients from the organic emitting layer (layer 0) to the half-spaces $j(j = 1, 2)$. k_{\parallel} and $k_{z,j}$ are the radial and z component of the wave vector k_j in the half-spaces j . With the use of the superposition of plane waves, the power W_1 radiated to the half-spaces $j(j = 1)$ can be written as an integral:

$$W_1 = \int_0^{+\infty} K_1(k_{\parallel}) dk_{\parallel}^2, \quad (\text{A2})$$

where K_1 is the power density per unit dk_{\parallel}^2 . Based on the polarity, we can separate the power density K_1 into s -polarized power density K_1^s and p -polarized power density K_1^p :

$$K_1(\theta, \phi) = K_1^s(\theta, \phi) + K_1^p(\theta, \phi), \quad (\text{A3})$$

where polar angle θ and azimuth angle ϕ are shown in FIG. 1(b) lower panel. For an electric dipole in the emitting layer, the s -polarized and p -polarized power densities radiated upward in $x - z$ plane per unit dk_{\parallel} read^{24,26}

$$K_1^s(\theta, \phi) = \frac{3}{8} \frac{1}{k_0 k_{z,0}} \frac{|1 + a_2^s|^2}{|1 - a^s|^2} T_1^s \sin^2 \theta \sin^2 \phi, \quad (\text{A4a})$$

$$\begin{aligned} K_1^p(\theta, \phi) &= \frac{3}{8} \frac{k_{\parallel}^2}{k_0^3 k_{z,0}} \frac{|1 + a_2^p|^2}{|1 - a^p|^2} T_1^p \cos^2 \theta, \\ &+ \frac{3}{8} \frac{k_{z,0}}{k_0^3} \frac{|1 - a_2^p|^2}{|1 - a^p|^2} T_1^p \sin^2 \theta \cos^2 \phi, \\ &- \frac{3}{8} \frac{k_{\parallel}}{k_0^3} \frac{1}{|1 - a^p|^2} T_2^p T_1^p \sin \theta \cos \phi, \end{aligned} \quad (\text{A4b})$$

where $a_{\pm}^{s,p}$ is given by

$$a_1^{s,p} = r_1^{s,p} \exp(2jk_{z,0}z_1), \quad (\text{A5a})$$

$$a_2^{s,p} = r_2^{s,p} \exp(2jk_{z,0}z_2), \quad (\text{A5b})$$

and $a^{s,p}$ is the product of $a_1^{s,p}$ and $a_2^{s,p}$

$$\begin{aligned} a^{s,p} &= a_1^{s,p} a_2^{s,p} \\ &= r_1^{s,p} r_2^{s,p} \exp(2jk_{z,0}d_0). \end{aligned} \quad (\text{A6})$$

According to the specific form of power densities given by Eq. (A4), p -polarized power density K^p can be further separated into three different parts K_1^p , K_2^p and K_3^p :

$$\begin{aligned} K_1^p(\theta, \phi) &= K_1^{p1}(\theta, \phi) + K_1^{p2}(\theta, \phi) \\ &+ K_1^{p3}(\theta, \phi), \end{aligned} \quad (\text{A7})$$

with

$$K_1^{p1}(\theta, \phi) = \frac{3}{8} \frac{k_{\parallel}^2}{k_0^3 k_{z,0}} \frac{|1 + a_2^p|^2}{|1 - a^p|^2} T_1^p \cos^2 \theta, \quad (\text{A8a})$$

$$K_1^{p2}(\theta, \phi) = \frac{3}{8} \frac{k_{z,0}}{k_0^3} \frac{|1 - a_2^p|^2}{|1 - a^p|^2} T_1^p \sin^2 \theta \cos^2 \phi, \quad (\text{A8b})$$

$$K_1^{p3}(\theta, \phi) = -\frac{3}{8} \frac{k_{\parallel}}{k_0^3} \frac{1}{|1 - a^p|^2} T_2^p T_1^p \sin \theta \cos \phi. \quad (\text{A8c})$$

For an emission angle α in half-space $j(j = 1)$, the power density $K_1^{s,p}$ per unit dk_{\parallel} can be transformed to a power density $P_1^{s,p}$ per solid angle. The power densities per solid angle of an arbitrarily distributed dipole ensemble can be written as

$$P_1^{s,p}(\theta, \phi) = \frac{k_1^2 \cos \alpha}{\pi} K_1^{s,p}(\theta, \phi), \quad (\text{A9})$$

-
- * Electronic address: lshi@fudan.edu.cn
- † Electronic address: jzi@fudan.edu.cn
- ¹ C. W. Tang and S. A. VanSlyke, [Appl. Phys. Lett.](#) **51**, 913 (1987).
 - ² H. Nakanotani, T. Higuchi, T. Furukawa, *et al.*, [Nat. Commun.](#) **5**, 4016 (2014).
 - ³ Y. Kim, H.-C. Jeong, S. H. Kim, *et al.*, [Adv. Funct. Mater.](#) **15**, 1799 (2005).
 - ⁴ D.-H. Kim, A. DAléo, X.-K. Chen, *et al.*, [Nat. Photonics](#) **12**, 98 (2018).
 - ⁵ M. A. Baldo, D. F. O'Brien, Y. J. You, *et al.*, [Nature](#) **395**, 151 (1998).
 - ⁶ M. A. Baldo, S. L. Lamansky, P. E. Burrows, *et al.*, [Appl. Phys. Lett.](#) **75**, 4 (1999).
 - ⁷ M. G. Helander, Z. B. Wang, J. Qiu, *et al.*, [Science](#) **332**, 944 (2011).
 - ⁸ K.-H. Kim and J.-J. Kim, [Advanced Materials](#) **30**, 1705600 (2018).
 - ⁹ R. Costa, G. Fernández, L. Sanchez, *et al.*, [Chemistry](#) **16**, 9855 (2010).
 - ¹⁰ C.-L. Lin, T.-Y. Cho, C.-H. Chang, *et al.*, [Sid Symposium Digest of Technical Papers](#) **37** (2006).
 - ¹¹ M. Fläemmich, M. Gather, N. Danz, *et al.*, [Appl. Phys. Lett.](#) **95**, 263306 (2009).
 - ¹² S. Nowy, B. Krummacher, J. Frischeisen, *et al.*, [J. Appl. Phys.](#) **104**, 123109 (2009).
 - ¹³ J. Frischeisen, D. Yokoyama, C. Adachi, *et al.*, [Appl. Phys. Lett.](#) **96**, 073302 (2010).
 - ¹⁴ W. Brütting, J. Frischeisen, T. Schmidt, *et al.*, [Phys. Status Solidi A](#) **210**, 44 (2013).
 - ¹⁵ M. Fläemmich, S. Roth, N. Danz, *et al.*, [Fraunhofer IOF](#) **7722**, 77220D (2010).
 - ¹⁶ T. Lampe, T. Schmidt, M. Jurow, *et al.*, [Chem. Mater.](#) **28**, 712 (2016).
 - ¹⁷ T. Komino, Y. Oki, and C. Adachi, [Sci. Rep.](#) **7**, 8405 (2017).
 - ¹⁸ H. Cho, C. W. Joo, B.-H. Kwon, *et al.*, [Org. Electron.](#) **62**, 72 (2018).
 - ¹⁹ Y. Hasegawa, Y. Yamada, M. Sasaki, *et al.*, [J. Phys. Chem. Lett.](#) **9**, 863 (2018).
 - ²⁰ R. Chance, A. Prock, and R. Silbey, [J. Chem. Phys.](#) **60**, 2744 (1974).
 - ²¹ W. Lukosz and R. Kunz, [J. Opt. Soc. Am.](#) **67**, 1607 (1977).

- ²² R. Chance, A. Prock, and R. Silbey, Molecular fluorescence and energy transfer near interfaces (2007) pp. 1 – 65.
- ²³ W. Lukosz, *Phys. Rev. B* **22**, 3030 (1980).
- ²⁴ W. Lukosz, *J. Opt. Soc. Am.* **71**, 744 (1981).
- ²⁵ G. Ford and W. Weber, *Phys. Rep.* **113**, 197 (1984).
- ²⁶ K. Neyts, *J. Opt. Soc. Am. A* **15**, 962 (1998).
- ²⁷ W. Barnes, *J. Mod. Optic.* **45**, 661 (1998).
- ²⁸ T. Schmidt, T. Lampe, D. M.R, *et al.*, *Phys. Rev. Appl.* **8**, 037001 (2017).
- ²⁹ D. Yokoyama, *J. Mater. Chem.* **21**, 19187 (2011).
- ³⁰ V. Sundar, J. Zaumseil, V. Podzorov, *et al.*, *Science* **303**, 1644 (2004).
- ³¹ T. Amaya, S. Seki, T. Moriuchi, *et al.*, *J. Am. Chem. Soc.* **131**, 408 (2009).
- ³² K. Baek, D.-M. Lee, Y.-J. Lee, *et al.*, *Light Sci. Appl.* **8**, 120 (2019).